Developmental Biology 318 (2008) 247–257

Contents lists available at ScienceDirect

Developmental Biology

journal homepage: www.elsevier.com/developmentalbiology

Larval cells become imaginal cells under the control of *homothorax* prior to metamorphosis in the *Drosophila* tracheal system

Makoto Sato *, Yusuke Kitada, Tetsuya Tabata

Laboratory of Morphogenesis, Institute of Molecular and Cellular Biosciences, University of Tokyo, 1-1-1 Yayoi, Bunkyo, Tokyo 113-0032, Japan

ARTICLE INFO

Article history:
Received for publication 28 November 2007
Revised 11 March 2008
Accepted 11 March 2008
Available online 27 March 2008

Keywords:
Metamorphosis
Repopulation
Reproliferation
Drosophila
Tracheal system
homothorax

ABSTRACT

In *Drosophila melanogaster*, one of the most derived species among holometabolous insects, undifferentiated imaginal cells that are set-aside during larval development are thought to proliferate and replace terminally differentiated larval cells to constitute adult structures. Essentially all tissues that undergo extensive proliferation and drastic morphological changes during metamorphosis are thought to derive from these imaginal cells and not from differentiated larval cells. The results of studies on metamorphosis of the *Drosophila* tracheal system suggested that large larval tracheal cells that are thought to be terminally differentiated may be eliminated via apoptosis and rapidly replaced by small imaginal cells that go on to form the adult tracheal system. However, the origin of the small imaginal tracheal cells has not been clear. Here, we show that large larval cells in tracheal metamere 2 (Tr2) divide and produce small imaginal cells prior to metamorphosis. In the absence of *homothorax* gene activity, larval cells in Tr2 become non-proliferative and small imaginal cells are not produced, indicating that *homothorax* is necessary for proliferation of Tr2 larval cells. These unexpected results suggest that larval cells can become imaginal cells and directly contribute to the adult tissue in the *Drosophila* tracheal system. During metamorphosis of less derived species of holometabolous insects, adult structures are known to be formed via cells constituting larval structures. Thus, the *Drosophila* tracheal system may utilize ancestral mode of metamorphosis.

Introduction

Metamorphosis of holometabolous insects provides separate larval and adult stages to adapt to distinct environments. In general, adult structures originate from larval structures in more ancestral species, while larval and adult structures have distinct developmental origins in more derived species (Svacha, 1992; Tanaka and Truman, 2005). Imaginal cells found among the most derived species are the adult primordia that are undifferentiated and set-aside during larval development and distinct from larval cells. The evolutional derivation of imaginal cells is a very important problem in the field of insect biology.

In *Drosophila melanogaster*, one of the most derived species among holometabolous insects, such imaginal cells are thought to proliferate and replace terminally differentiated larval cells during metamorphosis. With the exception of minorities of cells in central nervous system (e.g. mushroom body neurons) that are preserved in adults without cell proliferation (Lee et al., 1999), essentially all adult tissues result from extensive proliferation of imaginal cells during metamorphosis and not from differentiated larval cells. For example, imaginal discs grow without contributing to larval tissues but form the adult specific structures such as the head, thorax, wings and legs.

The *Drosophila* tracheal system is a tubular epithelial network that delivers oxygen to tissues throughout the body (Manning and Krasnow, 1993). The larval tracheal system is generated during embryogenesis, and has a bilaterally symmetric and rostrocaudally metameric network pattern. Like other tissues, the tracheal system is extensively remodeled during metamorphosis after late third instar stage. Prior to early third instar, all tracheal branches except the spiracular branches (SBs) are populated by large larval cells (Figs. 1A, C). In most branches of tracheal metamere 2 (Tr2) and in the dorsal branches (DBs) of more posterior metameres, larval cells are rapidly repopulated by smaller cells around mid third instar (24–26 h after the second molt; Figs. 1B, D, E) (Guha and Kornberg, 2005). Because imaginal cells that are set-aside during larval development are thought to form adult tissues during metamorphosis in *D. melanogaster*, imaginal tracheal cells may also reside somewhere in or near the larval tracheal branches. Indeed, the SBs have been thought to be the source of the imaginal tracheal cells that then spread or migrate along the larval tracheal system during metamorphosis (Manning and Krasnow, 1993; Matsuno, 1990). If this is the case, repopulation of Tr2 may take place sequentially, starting with cells closer to the SB. However, such a correlation was not obvious in a previous study (Guha and Kornberg, 2005).

A characteristic feature of the adult tracheal system is the air sacs, adult-specific tracheae that are juxtaposed with the flight muscles and the brain. In a previous study, the air sac primordium (ASP) was shown to arise during third larval instar from a wing-disc-associated larval

* Corresponding author. Present address: Frontier Science Organization, Kanazawa University, 13-1 Takaramachi, Kanazawa, Ishikawa 920-8641, Japan. Fax: +81 76 234 4239.
E-mail address: makotos@staff.kanazawa-u.ac.jp (M. Sato).

0012-1606/$ – see front matter © 2008 Elsevier Inc. All rights reserved.
doi:10.1016/j.ydbio.2008.03.025

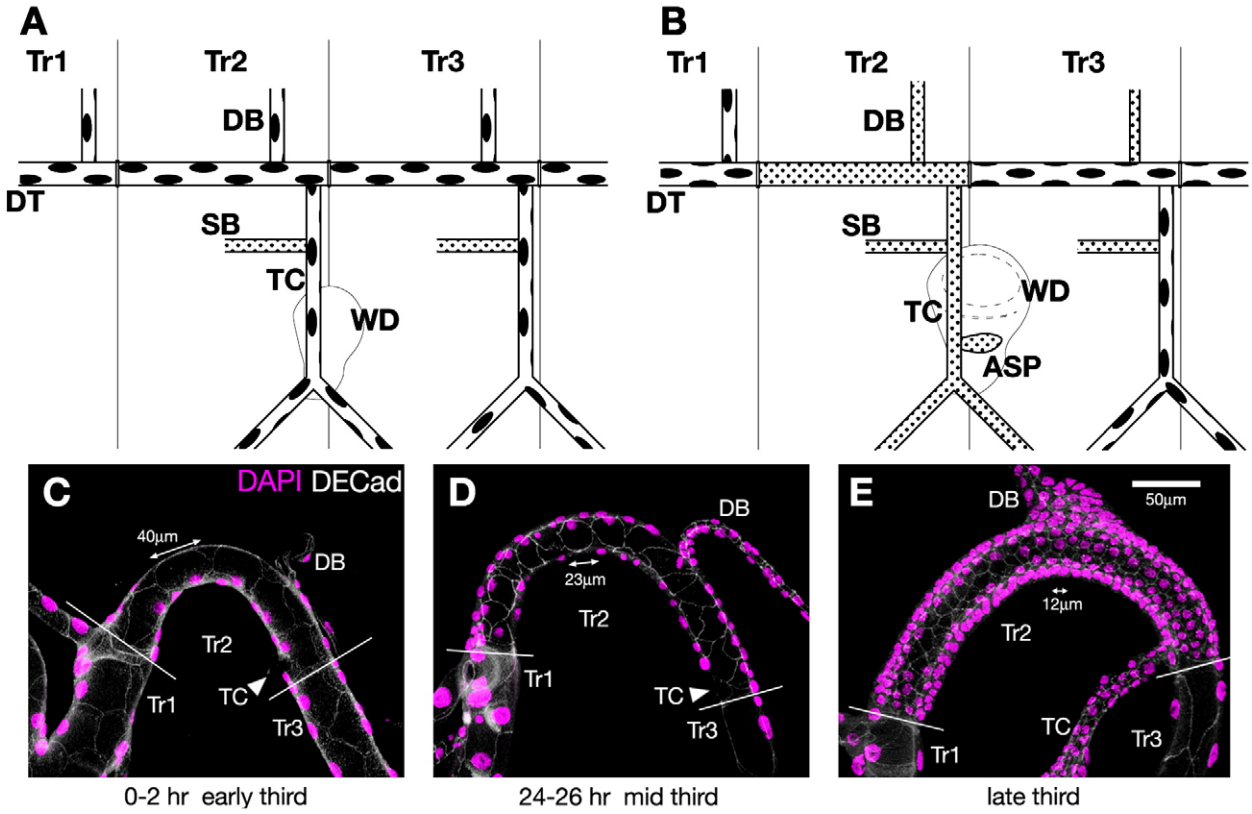

Fig. 1. Re-examining tracheal repopulation. (A, B) Schematic drawings of the thoracic tracheal metameres (A) before and (B) after repopulation. Small dots are nuclei of small proliferative cells, while large elliptic dots are nuclei of large larval cells. (C–E) Emergence of smaller cells during repopulation in the tracheal metamere Tr2. (C) At early third instar (0–2 h ASM), large cells of sizes comparable to Tr1/3 cells are found (typically ~40 μm). (D) At mid third instar (24–26 h ASM), cells of intermediate sizes are found (typically ~23 μm). (E) At late third instar (wandering larvae immediately before pupariation; roughly 40–48 h ASM), only small cells are found (typically ~12 μm). DAPI, magenta; DE-Cadherin, white. Anterior, left. Abbreviations: Tr1–3, tracheal metamere 1–3; DT, dorsal trunk; DB, dorsal branch; TC, transverse connective; SB, spiracular branch; WD, wing disc; ASP, air sac primordium. Scale bar, 50 μm.

tracheal branch, the transverse connective (TC; Figs. 1A, B), in the tracheal metamere Tr2 and to form air sacs in the adult thorax (Sato and Kornberg, 2002). After completion of repopulation, the small imaginal cells in Tr2 respond to Branchless (Bnl)-FGF expressed in the wing disc and migrate out of the branch, at which point they begin to proliferate and undergo morphogenesis (Sato and Kornberg, 2002).

To elucidate genetic mechanisms of repopulation and ASP growth, we carried out a tracheal system-specific RNAi screen to find that the *homothorax* gene is required for repopulation. Using *homothorax* as a genetic tool, the detailed mechanisms of repopulation were investigated. As a result, we revealed that larval cells in Tr2 are proliferative and rapidly divide to produce imaginal cells during repopulation. Thus, imaginal tracheal cells are the direct progeny of larval cells in the tracheal system. The imaginal cells then respond to FGF ligand by migrating out of the larval system to form completely novel structures in the adult, the air sacs (Sato and Kornberg, 2002). These unexpected results suggest that larval tracheal cells can become imaginal tracheal cells and directly contribute to the adult tissue in *D. melanogaster*, one of the most derived holometabolous insects. Since larval cells commonly contribute to adult structures in less derived insects (Svacha, 1992; Tanaka and Truman, 2005), the *Drosophila* tracheal system may utilize ancestral mode of metamorphosis. Similar strategy of metamorphosis may also be found in wide variety of holometabolous insects.

Materials and methods

Plasmid construction

BRG (btl>DsRed2, y⁺>Gal4)

The *Kpn*I–*Sac*I fragment of the *Gal4* cDNA in *pGaTN* was inserted into *pUC19*. The *Sma*I–*Xba*I fragment containing *Gal4* and the *Not*I–*Nde*I fragment of *P[ABP]* containing the *btl* promoter (Ohshiro and Saigo, 1997) were ligated and inserted between the *Not*I and *Xba*I sites of the *Carnegie4* vector. A flip-out cassette containing *DsRed2* and *yellow⁺* between two FRT sites (Sato and Kornberg, 2002) was inserted into the unique *Kpn*I site situated between the *btl* promoter and *Gal4*.

btl-flp

pCaSpeR4-SV40polyA was generated by inserting a synthetic DNA fragment containing *Eco*RI, *Not*I, *Bam*HI, *Bgl*II, *Hpa*I, *Kpn*I, *Sph*I and *Xba*I sites by replacing a fragment containing *tubulin* promoter and *Gal80* situated between *Eco*RI and *Xba*I sites of the *pCaSpeR4* vector containing *tubulin* promoter-*Gal80*-SV40 polyA (Lee and Luo, 1999). The *Not*I–*Bgl*II fragment of *p[ABP]* containing the *btl* promoter was inserted between the *Not*I and *Bgl*II sites upstream of SV40 polyA. The *Kpn*I–*Xba*I fragment containing the *FLPase* cDNA in *pBD927* (a gift from Barry Dickson) was inserted into the *Kpn*I and *Xba*I site between the *btl* promoter and SV40 polyA.

Fly strains

UAS-hthIR (NIG-FLY, Mishima, Japan), *UAS-Meis1, hth^{P2} FRT82B* (Rieckhof et al., 1997), *UAS-exdIR* (VDRC, Vienna, Austria), *Ubx^{1} FRT82B* (Fly Base), *btl-Gal4, UAS-GFP* (Sato and Kornberg, 2002), *actin-Gal4* is a derivative of *AyGal4* (Ito et al., 1997), *hs-flp, tubulinP-Gal80 FRT82B, FRT82B, UAS-CD8GFP* (Lee and Luo, 1999), *fzr-lacZ* (Sigrist and Lehner, 1997), *UAS-p35, UAS-dronc^{DN}, UAS-DIAP1* (Igaki et al., 2002), *dronc$^{\Delta 2C8}$* (Kondo et al., 2006), *UAS-dacapo* (Lane et al., 1996). *btl-flp* was used to induce wild type, *hth^{P1}* and *Ubx^{1}* MARCM clones during embryogenesis.

Histochemistry

The following antibodies and materials were used and samples were mounted in Vectashield mounting media containing DAPI (Vector Laboratories): rat anti-DECad (Developmental Study Hybridoma Bank), rabbit anti-CycA (Nakato et al., 2002), rabbit anti-phospho Histone-H3 (Upstate Biotechnology), rabbit anti-Hth (Kurant et al., 1998), mouse anti-Ubx FP3.38 (White and Wilcox, 1984), rabbit anti-cleaved Caspase3 (Cell Signaling Technology), mouse anti-LacZ (Promega), donkey anti-mouse/rat Cy3/Cy5 (Jackson ImmunoResearch), goat anti-rabbit Alexa 546/660, rabbit anti-GFP Alexa 488 and TOTO-3 (Invitrogen). Tracheal images were 3D reconstructed using Zeiss LSM510 software.

DAPI fluorescence quantification

btl-Gal4 UAS-GFP larvae were dissected and fixed in 4% formaldehyde for 30 min and washed in PBT. Rinsed in PBS, larval tracheae were mounted in Vectashield containing DAPI (Vector Laboratories) and incubated at 4 °C for a week. DAPI fluorescence images for sequential non-overlapping confocal sections were captured as 12 bit images using Zeiss LSM 510. 20× and 40× objective lenses were used for early third and first/second instar samples, respectively. For each one of tracheal cell, signal intensities of sequential confocal sections were integrated along Z-axis to obtain DAPI fluorescence value for a single nucleus using ImageJ 1.36b software.

Results

Cells of intermediate size are found during repopulation

In an attempt to determine the origin of the imaginal tracheal cells that go on to form the air sac primordium (ASP), we re-examined the process of repopulation during third instar. The focus of our work was primarily on the major tracheal branches or dorsal trunks (DTs) in tracheal metamere 2 (Tr2; Figs. 1A, B). Essentially the same results were obtained for other branches, including the dorsal branches (DBs) and the transverse connectives (TCs). Prior to repopulation at early third instar (0–2 h after the second molt (ASM); Fig. 1C), Tr2 is comprised of large cells that are comparable in size to the cells in Tr1/3 (~40 μm). After completion of repopulation at late third instar (roughly 40–48 h ASM, immediately before pupariation; Fig. 1E), Tr2 is comprised of very small cells (~12 μm). The results are consistent with the earlier study (Guha and Kornberg, 2005). However, if the large cells were directly replaced by small cells as suggested by Guha and Kornberg, Tr2 would be comprised of the mixture of small and large cells just after the beginning of repopulation. Surprisingly, we found instead that Tr2 is mainly comprised of cells of intermediate size (~23 μm) at mid third instar (24–26 h ASM; Fig. 1D). This observation has not been reported by Guha and Kornberg, and may suggest the process of repopulation is not merely the replacement of large larval cells by small imaginal cells.

Apoptosis may not be essential for repopulation

It has previously been suggested that elimination of larval cells via apoptosis may be prerequisite for the replacement of larval cells with imaginal cells in Tr2 (Guha and Kornberg, 2005). We tested this idea by looking at an apoptotic marker, an antibody against cleaved Caspase3, in cells present in the Tr2 branches before and after repopulation. Surprisingly, apoptotic activity was only detected after repopulation was complete (arrows in Fig. 2C), not before or during repopulation (Figs. 2A, B). No Caspase3 signal was detected at 0–4, 4–8, 8–12, 12–16, 16–20, 20–24, 24–28, 28–32 and 32–36 h ASM, while strong signal was detected in wandering late third instar larvae at 36–40 h ASM (not shown).

To examine a possible role for apoptosis in the process, cell death was artificially inhibited by expressing *p35* in the tracheal cells (Zhou et al., 1997). Whereas apoptosis was suppressed (i.e. we observed a lack of staining with anti-cleaved Caspase3 antibody) neither repopulation (Fig. 2D) nor ASP growth (arrow in Fig. 2E) was significantly compromised. Note that Caspase3 activation is suppressed in tracheal cells, but not in surrounding non-tracheal cells (arrowheads in Fig. 2E). Moreover, significant defects were hardly induced in flies with a mutation in Dronc, an initiator caspase required for apoptotic signals, or by inhibiting apoptosis via ectopic expression of DIAP1, an apoptosis inhibitor, or a dominant-negative form of Dronc (not shown) (Igaki et al., 2002; Kondo et al., 2006). These results strongly suggest that apoptosis plays only a small role if any during repopulation, and that large larval cells disappear mostly via an as yet unknown mechanism. Guha and Kornberg expressed *hid* double-stranded RNA transgene under the control of the heat shock promoter to inhibit apoptosis and reported that *hid*-dependent apoptosis is necessary for repopulation (Guha and Kornberg, 2005). Their conclusions may have been caused by off-target effects of RNAi or by general growth arrest of larvae due to ubiquitous expression of the transgene.

homothorax is required for repopulation and ASP growth

To understand the mechanisms of tracheal repopulation and ASP migration, we searched for genes specifically required for ASP growth by a tissue-specific RNAi screen using a trachea-specific Gal4 driver under the control of *breathless* promoter (*btl-Gal4*) (Ohshiro and Saigo, 1997; Shiga et al., 1996) and UAS-inverted repeat strains (UAS-IR) provided by NIG-FLY, Japan. Defects in ASP growth were examined by

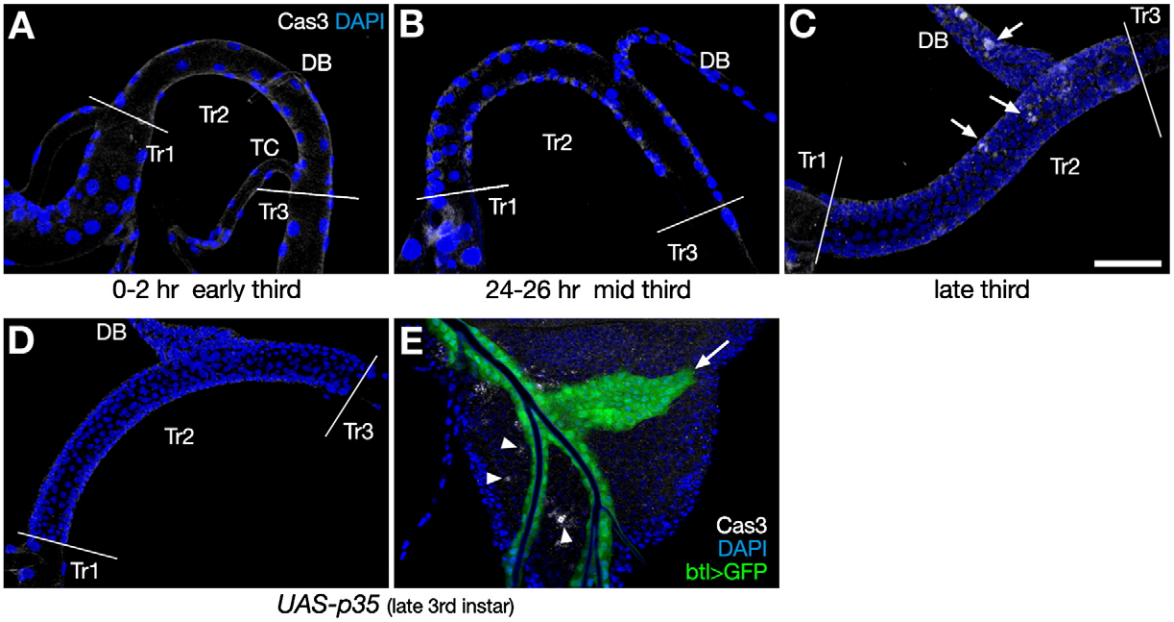

Fig. 2. Apoptosis plays only minor roles during repopulation. (A–C) Caspase3 activation is detected in small cells after the completion of repopulation at late third instar (C; arrows), but not in earlier stages (A, B). (D, E) Inhibition of apoptosis by expressing *UAS-p35* under the control of *btl-Gal4* does not compromise either (D) repopulation or (E) ASP growth (arrow) at late third instar. Caspase3 activation is suppressed in tracheal cells, but not in surrounding non-tracheal cells (arrowheads in panel E). Cleaved Caspase3, white; DAPI, blue; GFP, green. Scale bar, 50 μm.

visualizing tracheal cells with *UAS-GFP* under the control of *btl-Gal4*. Among 2708 strains examined, 1699 strains showed defects including embryonic or larval lethality in 268 strains. Various defects in ASP growth such as reduction, expansion, split branch, dissociated cells, irregular morphology, spiky shape, thin branch and misrouting were observed in 312, 17, 61, 150, 120, 32, 11 and 1 strains, respectively. However, penetrance or expressivity of the above defects was not strong in general. Or, strong defects were frequently associated with non-specific defects in the main tracheal branch (TC). UAS-IR strains for *homothorax* (*hth*) gene, which encodes a conserved homeobox transcription factor (Kurant et al., 1998; Pai et al., 1998; Rieckhof et al., 1997), were the only strains that caused complete loss of ASP branches but did not affect the morphology of the other tracheal branches (Figs. 3A, C; 100% penetrant). Additionally, a closer examination revealed that cells in the tracheal metamere Tr2 remain large at late third instar, suggesting that repopulation does not take place in the absence of *hth* function (Figs. 3A–D; 100% penetrant). Note that all of the cells along the DT, DB and TC branches in Tr2 are as large as cells in Tr1/3 at late third instar. Repopulation in DBs in more posterior metameres was also inhibited (not shown). Since *btl-Gal4* is expressed in all the tracheal cells except for those in spiracular branches (SBs; Figs. 1B and 3A) and *hth* acts cell-autonomously (see below), these defects are not caused by the loss of *hth* functions in SBs, and cells in SBs may not be responsible for repopulation in a wild type background. The loss of the ASP phenotype induced by *hth*-knockdown may be a secondary defect due to the loss of repopulation, as repopulation takes place prior to ASP growth in a wild type background (see below).

To exclude the possibility of off-target effects of RNAi, rescue experiments were carried out by co-expressing *Meis1*, a human orthologue for *hth* (Kurant et al., 1998; Rieckhof et al., 1997). The defects in repopulation and ASP growth induced by *UAS-hthIR* were significantly suppressed by co-expression of *UAS-Meis1* (Figs. 3E, F), suggesting that *hth* is indeed responsible for the defects described above. The degree of rescue varied from partial to nearly complete among individuals. In the example shown in Fig. 3F, only part of Tr2 is populated by small cells (arrows). Intriguingly, islands of small cells isolated by surrounding large cells were occasionally found along rescued Tr2 branches (Fig. 3F).

If small cells in Tr2 are supplied by particular sources, such as cells that migrate from SBs, abrupt occupation of tracheal branches by ectopic larval cells might block migration of small imaginal cells. Alternatively, the presence of ectopic larval cells may uncover the presence of small cells as they migrate on the surface of the large cells. Thus, we generated clones of *hth* mutant cells to induce formation of ectopic large larval cells that occupy part of the tracheal branches at late third instar. In Figs. 3G and H, ectopic larval cells are autonomously generated in the middle of the TC and DT branches, respectively, which might prevent small imaginal cells from migrating along the branches. However, the regular arrangement of small cells and ASP growth were not disrupted by the presence of ectopic large cells (Figs. 3G, H). Moreover, migrating small cells were not detected on the surface of large cells. The results do not support the classical model that small imaginal cells are supplied via migration or spreading along the tracheal branches (Manning and Krasnow, 1993; Matsuno, 1990).

Tr2 cells may remain diploid while Tr1/3 cells endoreplicate during larval development

As described earlier, cells of intermediate size are detectable along Tr2 branches in the course of repopulation (Fig. 1D). Hence, we assumed that repopulation is not a global event accompanied by migration of small cells but instead, is a fairly local event, such as one occurring via on-site cell division accompanied by decrease in cell size. However, larval cells with large nuclei are usually in endocycles and are thought to be non-proliferative, and consistent with that idea, cells in Tr2 are morphologically very similar to large cells in other tracheal metameres prior to repopulation (Fig. 1C). Here, we were forced to call into question the assumption that large larval cells in Tr2 are endoreplicating and non-proliferative and ask if instead, the large cells in Tr2 may be in a cell cycle state that is distinct from that of large larval cells in other metameres.

fizzy-related (*fzr*) is expressed in non-proliferative, endocycling cells, whereas CyclinA (CycA) is expressed in proliferative cells that undergo normal mitotic cycles. Additionally, CycA is known to accumulate during G2 phase (Lehner and O'Farrell, 1990; Schaeffer et al., 2004; Sigrist and Lehner, 1997). We examined the cell cycle state of larval cells in the tracheal metameres Tr1, Tr2 and Tr3 at second instar using *fzr-lacZ* and CycA as markers (Figs. 4A, B). Since larval cells in Tr1 and Tr3 expressed *fzr* but not CycA, they are regarded as non-proliferative endoreplicating cells as expected (Fig. 4A). Surprisingly, however, in Tr2 larval cells along DTs, CycA expression was up-regulated whereas *fzr* was significantly down-regulated as compared with cells in the other tracheal metameres (Fig. 4A), suggesting that large cells in Tr2 are proliferative diploid cells in G2 phase that probably contain 4C DNA content and undergo normal mitotic cycles. Endoreplicating cells contain significantly larger amount of DNA compared to cells in normal mitotic cycles. To address if Tr2 cells contain significantly lower amount of DNA compared to Tr1/3 cells, DAPI fluorescence intensity was quantified for nuclei in wild type DT cells in Tr1, Tr2 and Tr3 at early third instar (0–4 h ASM). As shown in Fig. 4C, Tr2 cells showed about a third of relative DAPI fluorescence intensity compared to Tr1/3 cells, suggesting that Tr2 cells contain significantly lower amount of DNA prior to repopulation. Consistently, sizes of nuclei in Tr2 are somewhat smaller than in Tr1/3 (average length of longer diameter of nuclei in Tr1, Tr2 and Tr3 was 13.9 (S.D.=1.4), 10.0 (S.D.=0.9) and 12.0 μm (S.D.=1.1), respectively). The nuclear size may reflect amount of DNA contained in a nucleus.

The above data suggest Tr1/3 cells endoreplicate to gain significantly higher amount of DNA prior to third larval instar. Indeed, DAPI fluorescence values in Tr2 and Tr1/3 cells were discrete as early as second instar (Fig. 4D). Although the separation of the spectra was not clear, Tr1/3 cells tended to show stronger fluorescence values than Tr2 cells at first instar (Fig. 4E). Thus, DNA content in Tr1/3 cells may be rapidly increased due to endoreplication during first instar, and as a result, the spectra of DNA content in Tr2 and Tr1/3 cells may be clearly separated at second instar. Since CycA was expressed in Tr2 at second instar (Fig. 4A) while *fzr* expression was not detected in Tr2 prior to repopulation (Figs. 4A and 7A, B), Tr2 cells are thought to remain diploid throughout larval development. Indeed, Tr2 cells tend to contain lower amount of DNA than Tr1/3 cells at first, second and early third instar (Figs. 4C–E).

As shown earlier, *hth*-knockdown inhibits repopulation in Tr2 (Fig. 3D). Thus, *hth* may be required to keep Tr2 cells in normal mitotic cycles and its absence may convert Tr2 cells to a non-proliferative state and indeed, the evidence is consistent with this idea. When *UAS-hthIR* was used to reduce *hth* levels, CycA expression was down-regulated and *fzr* expression was up-regulated in Tr2 larval cells (Fig. 4B). Thus, *hth* appears to facilitate repopulation by providing or maintaining proliferative potential in Tr2 larval cells.

Large larval cells sequentially divide to produce small imaginal cells

To address if large larval cells in Tr2 indeed divide to produce small imaginal cells, anti-phospho Histone H3 antibody was used to detect cells in M phase in the course of repopulation. Consistent with CycA expression, a strong pH3 signal was detected in large larval cells in Tr2 at mid third instar (16–18 h ASM; Fig. 5A). Twin pH3-positive nuclei were occasionally found in large cells in anaphase (arrowheads in Fig. 5A). Note that a cell of intermediate size (~23 μm) was found adjacent to large cells (~40 μm). No pH3 positive cell was found in Tr2 at 12–14 h ASM (n=6) but pH3 signals were frequently detected

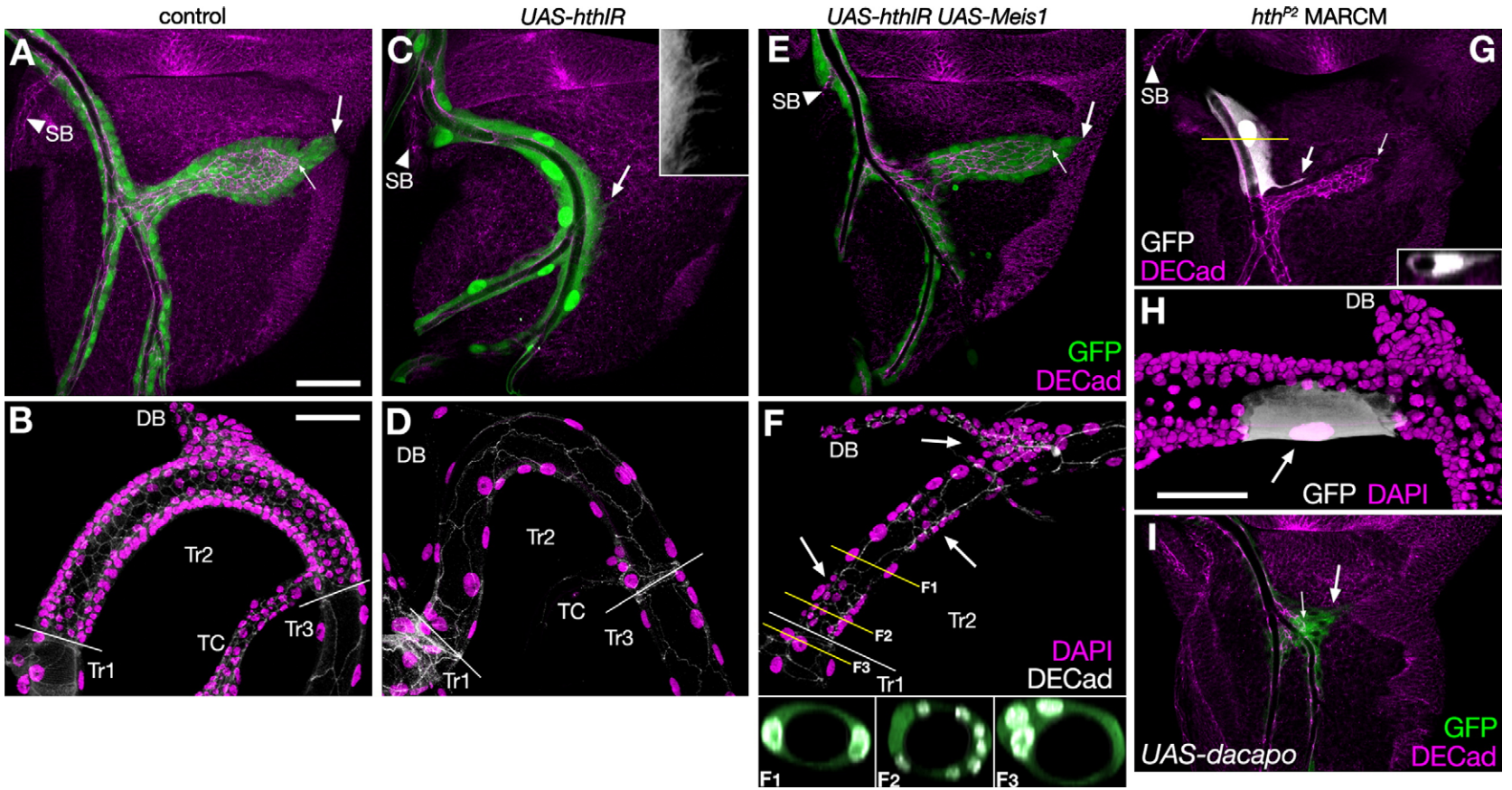

Fig. 3. *homothorax* is required for repopulation and ASP growth. (A–F) Repopulation and ASP growth are inhibited by *hth*-knockdown, but are rescued by co-expressing *Meis1*. (A, B) In control flies, ASPs migrate to the posterior edge of the wing disc (arrows in A) and only small cells are found in Tr2 (B). (C, D) *hth*-knockdown in the tracheal system by *UAS-hthIR* under the control of *btl-Gal4* completely eliminated ASP growth (arrow in panel C), and transformed small cells into large cells in Tr2 (C, D). (C) Filopodia extending from large cells are magnified in the inset. (E, F) *UAS-Meis1* expression together with *UAS-hthIR* rescued ASP growth (arrows in panel E) and repopulation in Tr2 (arrows in panel F). (F) Sections at yellow lines are shown in (F1–3), showing an island of small cells is isolated by surrounding large cells. (G, H) Cell-autonomous inhibition of repopulation in *hth* mutant clones labeled with GFP. hth^{P2} clones were recovered as ectopic large cells among wild type small cells. (G) Note that the ASP branch is completely separated from the SB by the presence of an ectopic large cell as shown by a section at the yellow line (inset). The ectopic large cell projects filopodia toward the presumptive source of Bnl-FGF (arrows). (H) Note that regular arrangement of small cells is not perturbed by the presence of an ectopic large cell. (I) *UAS-dacapo* is expressed in clones labeled with CD8GFP. ASP growth is significantly reduced. All samples are of late third instar. (A, C, E, G, I) ASPs and tracheal branches associated with the dorsal part of the wing discs are shown. Filopodia and apical ridges of ASP cells are indicated by large and small arrows, respectively. DE-Cadherin, magenta; GFP, green or white. (B, D, F, H) DTs in the tracheal metamere Tr2 are shown. DAPI, magenta; DE-Cadherin, white (B, D, F); DAPI, magenta; GFP, white (H). DAPI, white; GFP, green (F1–3). Scale bars, 50 μm.

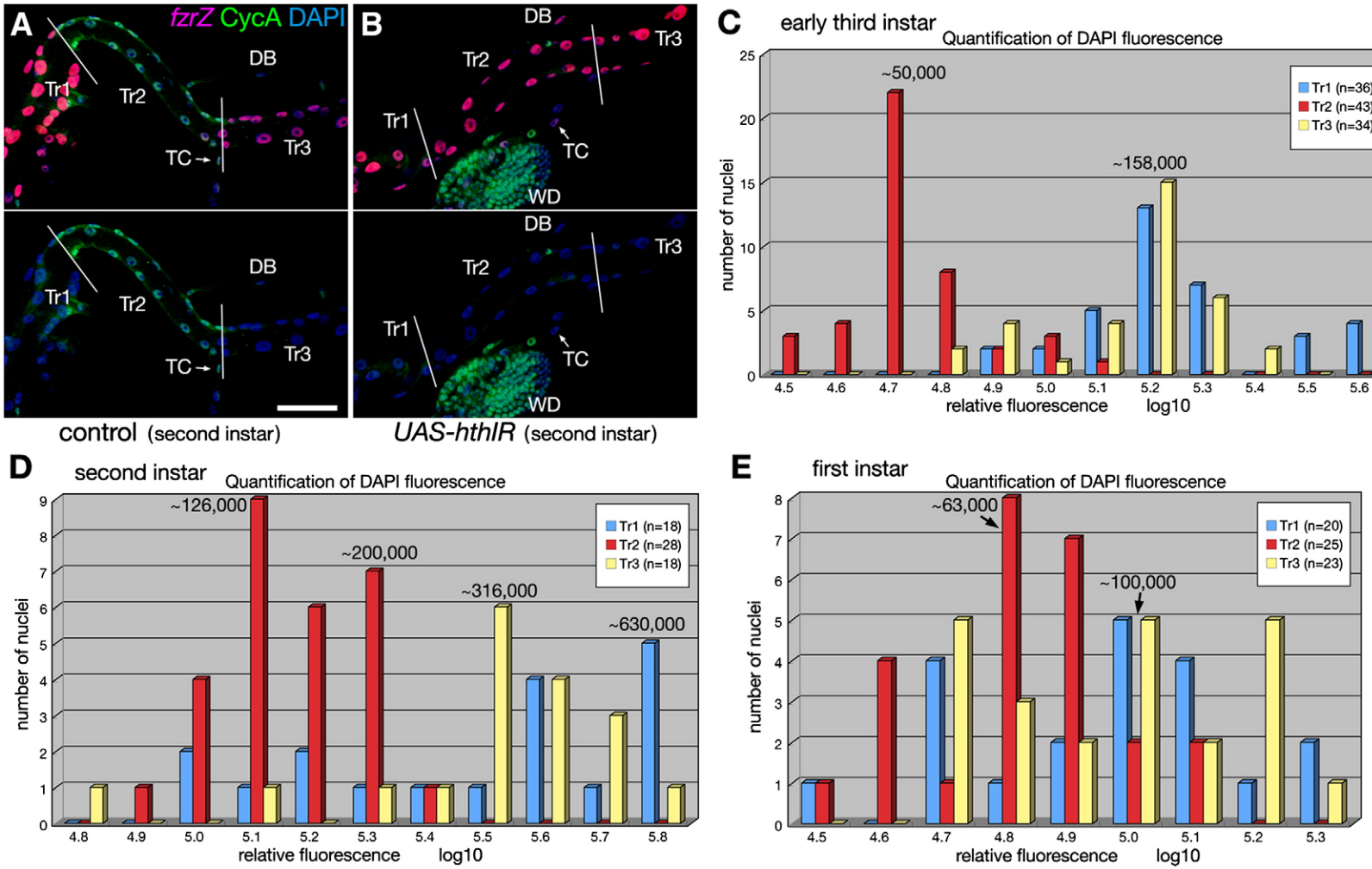

Fig. 4. Tr2 cells remain diploid while Tr1/3 cells endoreplicate during larval development. (A, B) *fzr-lacZ* (magenta) and CycA (green) expression in large cells along DT is visualized at second instar. All nuclei are labeled with DAPI (blue). Only CycA and DAPI are shown in the bottom panels. (A) In control flies, *fzr* is down-regulated while CycA is up-regulated in Tr2, suggesting Tr2 cells are proliferative diploid cells. (B) In flies expressing *UAS-hthIR* under the control of *btl-Gal4*, *fzr* expression is induced while CycA expression is abolished in Tr2, suggesting Tr2 became non-proliferative. Scale bar, 50 μm. (C–E) Histograms showing quantified DAPI fluorescence values of nuclei in wild type DT cells in Tr1 (blue), Tr2 (red) and Tr3 (yellow) at (C) early third instar (0–4 h ASM), (D) second instar and (E) first instar. The *X*-axes represent relative fluorescence values in logarithms, while *Y*-axes represent number of nuclei. (C) At early third instar, Tr2 and Tr1/3 cells show discrete fluorescence values with peaks around 50,000 and 158,000, respectively. (D) DAPI fluorescence values in Tr2 and Tr1/3 cells are also discrete at second instar. (E) At first instar, distributions of fluorescence values in Tr2 and Tr1/3 cells are not clearly discrete. However, Tr1/3 cells tend to show stronger fluorescence values than Tr2 cells.

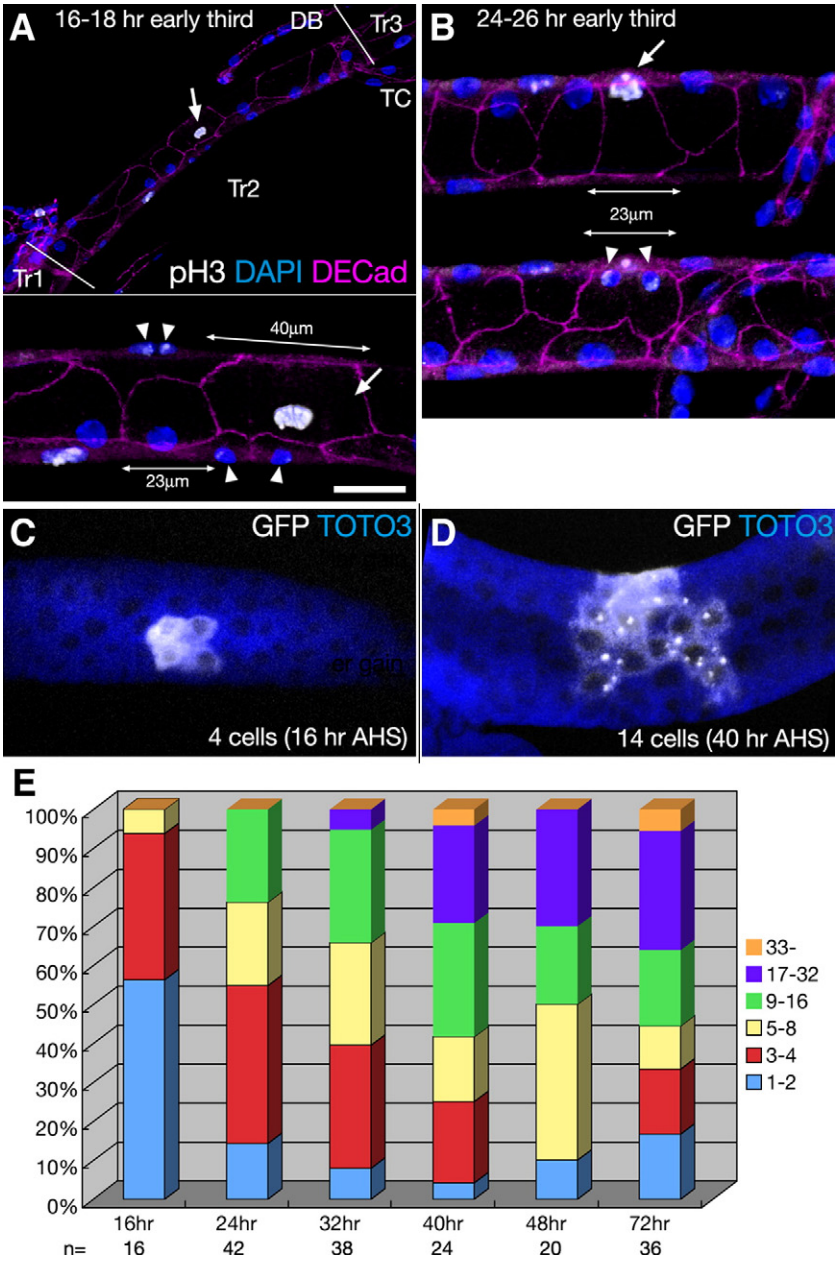

Fig. 5. Large larval cells sequentially divide to produce small imaginal cells. (A, B) Cells in M phase are visualized with anti-pH3 antibody (white) during mid third instar. Strong pH3 signals are observed in single large nuclei (arrows) and twin nuclei (arrowheads). DE-Cadherin, magenta; DAPI, blue. (A) Large larval cells enter M phase and divide at the onset of repopulation (16–18 h ASM). 3× magnified view is shown in the bottom panel. (B) Cells of intermediate size enter M phase to produce smaller cells (24–26 h ASM). (C, D) CD8GFP-positive clones were induced by a pulse of heat shock and progenies of putative single larval cells were visualized at late third instar. In typical examples, 4 and 14 cells were contained in clones examined at (C) 16 and (D) 40 h after the heat shock, respectively. *BRG UAS-CD8GFP* (white), TOTO-3 (blue). TOTO-3 strongly stains cytoplasm of tracheal cells with unknown reasons, and visualizes location of nuclei. Scale bar, 50 μm for (A) and 17.5 μm for (A–D). (E) A bar chart visualizing number of cells contained in single clones observed at late third instar at 16, 24, 32, 40, 48 and 72 h after the heat shock. The *Y*-axis shows percentages of clones containing 1–2, 3–4, 5–8, 9–16, 17–32 and 33< cells for each experiment.

in the following 2 h (n=15/18). Thus, repopulation begins after the onset of mitosis at 14–16 h ASM in DTs in Tr2. pH3 signals were continuously found in later stages until pupariation (about 40–48 h ASM), suggesting that larval cells divide several times to produce many cells. Interestingly, twin pH3-positive nuclei were found in cells of intermediate size at 24–26 h (Fig. 5B). Thus, the estimated doubling time of DT cells in Tr2 might be roughly 8 h, since large cells and their presumptive direct progenies enter anaphase at 16–18 and 24–26 h, respectively (Figs. 5A, B). However, pH3-negative DT cells were also frequently observed in Tr2 at the same time (Figs. 5A, B). They might divide non-synchronously and rather stochastically. As pH3 positive cells were detected in DB/TC branches in Tr2 as early as 8–10 h, the timing of repopulation may vary among branches (not shown). The pH3 signals were eliminated in Tr2 branches by *hth*-knockdown, with the exception of SBs, at mid third instar (16–18 h; not shown).

If large cells in Tr2 are proliferative, how many cells are produced from a single larval cell? To address this issue, the progeny of single larval cells in Tr2 were labeled with membrane-bound CD8GFP by inducing somatic recombination using a flip-out *Gal4* construct under the control of the *btl* promoter. Although except for SB cells, tracheal cell divisions were thought to be restricted to embryogenesis (Samakovlis et al., 1996), we found that Tr2 larval cells divide again during third instar (Figs. 5A, B). Therefore, clones induced after the onset of repopulation should contain smaller number of cells, while clones induced prior to repopulation should contain maximum

number of cells. CD8GFP-positive clones were induced by a pulse of heat shock at various stages during larval development and late third instar larvae were dissected at 16, 24, 32, 40, 48, 72 h after the heat shock (AHS). Number of CD8GFP-positive DT cells in isolated clones was counted (Figs. 5C–E). The clustered distributions of GFP positive cells may suggest Tr2 cells do not migrate or spread extensively (Figs. 5C, D). Since number of GFP-positive cells in a clone significantly varied even in the same experimental condition, clone size was classified into six categories based on number of cells contained (1–2, 3–4, 5–8, 9–16, 17–32 and 33–cells). Interestingly, clones examined at 16, 24 and 32 h AHS contained progressively larger number of cells (Fig. 6E). Since third larval instar persists for about 40–48 h and DT cell division in Tr2 begins at 16–18 h ASM (Fig. 5A), these clones are thought to be induced after the onset of repopulation during third larval instar. In contrast, clones induced prior to repopulation and examined at 40, 48 and 72 h AHS contained similar number of cells (Fig. 6E). These results are consistent with the model that Tr2 tracheal cells stop proliferation after embryogenesis, but re-proliferate in the course of repopulation during third larval instar. In general, single larval cells seem to produce roughly about 3 to 32 cells (Fig. 5E). Such a significant diversity may be due to stochastic nature of tracheal cell division (Figs. 5A, B) and apoptosis detected at late third instar (Fig. 2C).

Hth and Exd are not instructive cues that trigger repopulation in Tr2

Because Hth is expressed in all tracheal metameres before and after repopulation (Figs. 6A, B), it may play permissive rather than instructive roles. Extradenticle, an essential cofactor for Hth, was also uniformly expressed in all tracheal metameres (Figs. 6C, D) (Kurant et al., 1998; Pai et al., 1998; Rieckhof et al., 1997). Since *exd*-knockdown caused defects in repopulation and ASP growth indistinguishable from that caused by *hth*-knockdown (Figs. 6E, F and 3C, D), Exd may act in concert with Hth in the tracheal system as reported in the other developmental contexts (Kurant et al., 1998; Pai et al., 1998; Rieckhof et al., 1997). Thus, the Hth/Exd complex is thought to play permissive roles and additional factors may act in concert to provide instructive cues that keep Tr2 cells in normal mitotic cycles.

Instructive cues that may act in concert with Hth to regulate repopulation

What are the instructive cues that specify the cell-cycle state in Tr2? The best candidates would be Hox proteins, which specify the homeotic state of epidermal cells in each parasegment (PS) of embryo (Lewis, 1978) and are known to form complexes with Hth/Exd to regulate target gene expression (Ryoo et al., 1999). Tracheal

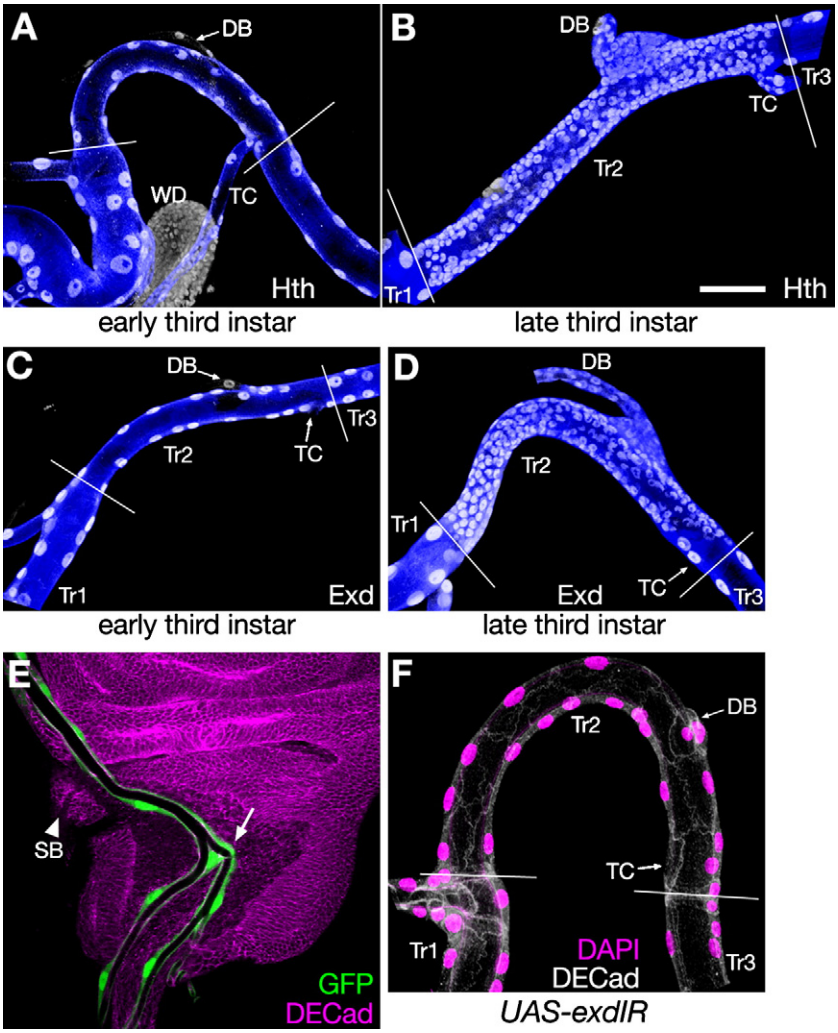

Fig. 6. Hth and Exd play permissive roles in repopulation. (A, B) Hth is uniformly expressed in Tr1/2/3 cells (A) before and (B) after repopulation. Hth, white; *btl-Gal4 UAS-GFP*, blue. (C, D) Exd is also uniformly expressed in Tr1/2/3 cells (C) before and (D) after repopulation. Exd, white; *btl-Gal4 UAS-GFP*, blue. (E, F) *exd*-knockdown in the tracheal system by *UAS-exdIR* under the control of *btl-Gal4* caused defects indistinguishable from that caused by *hth*-knockdown. ASP growth is completely abolished (arrow in panel E), and small cells are transformed into large cells in Tr2 (F). (E) DE-Cadherin, magenta; GFP, green. (F) DAPI, magenta; DE-Cadherin, white. Scale bar, 50 μm.

metameres Tr1, 2 and 3 are formed by invagination of tracheal primordial cells in PS4, 5 and 6, respectively. Among Hox proteins, Antennapedia (Antp) and Ultrabithorax (Ubx) are expressed in PS4/5 and PS6, respectively. However, the Tr2 fate cannot be specified by Antp expression in PS5 since Ubx is expressed in the region around the tracheal primordia in PS5 where Antp is repressed prior to tracheal invagination (Martinez-Arias et al., 1993). From this stage onward, Ubx is expressed in both Tr2 and Tr3 throughout larval development (Figs. 7A, B). Intriguingly, *Ubx* appears to have distinct roles in Tr2 and Tr3 as revealed by generating clones homozygous for an amorphic allele of *Ubx*. In addition to occasional ectopic repopulation found in Tr3 as reported in a previous study (Guha and Kornberg, 2005), ectopic large cells were induced in Tr2 (Figs. 7C, D). Since Ubx was the only Hox protein detected in Tr2 and Tr3 during second to early third instar (not shown), an additional instructive cue may act in concert with Ubx and Hth/Exd to provide Tr2 cells with a proliferative state, probably via activation of CycA expression with concurrent repression of *fzr* (Fig. 7E). Further study will be needed to elucidate complicated genetic mechanisms that distinguish the homeotic identity of Tr2 from that of Tr3. In addition to the spatial cues, hormonal signals such as ecdysteroids may provide temporal cues that trigger cell divisions of larval cells during third instar.

Involvement of cell division in ASP cell migration

Cell division is coupled to cell migration during mammalian branching morphogenesis but during *Drosophila* embryogenesis, tracheal cells migrate in the absence of cell divisions (Metzger and Krasnow, 1999). As cell proliferation is associated with ASP migration, ASP growth may be an excellent model for study of the mechanisms of proliferation-coupled cell migration (Cabernard and Affolter, 2005; Sato and Kornberg, 2002).

The complete loss of ASP growth in *hth*-knockdown flies may suggest that cell division is necessary for normal cell migration (Fig. 3C). Interestingly, even in the absence of *hth* function, filopodia-like structures extended from large cells toward the presumptive source of Bnl-FGF in the wing disc (Figs. 3C, G), suggesting that non-proliferative large cells lacking *hth* function still have potential to respond to Bnl-FGF by extending filopodia. However, cell division may be required to accomplish normal migration. To test this idea, we artificially inhibited cell proliferation of small imaginal cells associated with the wing disc by expressing Dacapo, a cyclin-dependent kinase inhibitor (de Nooij et al., 1996; Lane et al., 1996). Clones expressing *UAS-dacapo* were induced at early third instar using a flip-out *Gal4* construct under the control of the *btl* promoter. As a result of Dacapo expression, ASP migration was significantly delayed at late third instar (Fig. 3I), suggesting that normal cell division is necessary for completion of ASP migration.

Discussion

During metamorphosis of *D. melanogaster*, most adult tissues result from extensive proliferation of imaginal cells with the exception of minorities of cells in central nervous system (e.g. mushroom body neurons) that are preserved in adults without cell proliferation (Lee et al., 1999). In many cases, such imaginal cells have been believed to be set-aside during larval development and distinct from larval cells. For example, imaginal discs grow without contributing to larval tissues

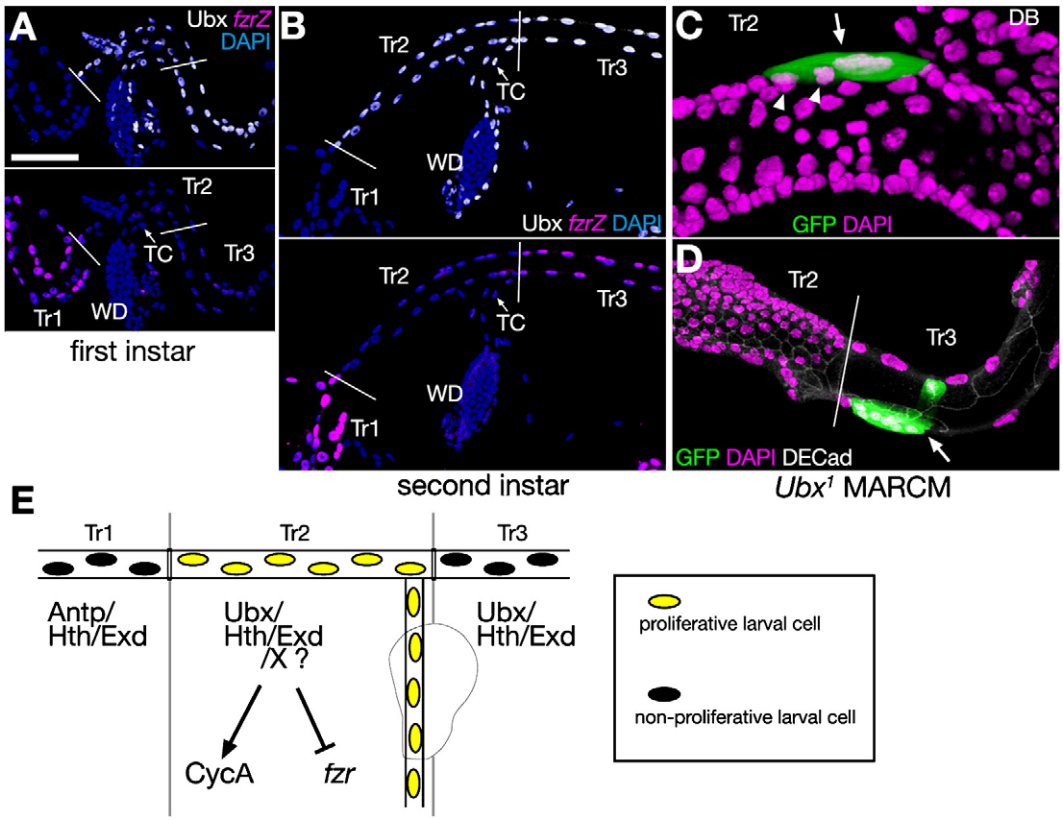

Fig. 7. Possible roles of Hox proteins in repopulation. (A, B) Ubx is expressed in both Tr2 and Tr3 cells during larval development. *fzr* is up-regulated in Tr1 cells during first instar (A) and then in Tr3 cells during second instar (B). Ubx, white; *fzr-lacZ*, magenta; DAPI, blue. (C, D) Distinct roles of *Ubx* in Tr2 and Tr3 as visualized by Ubx^1 homozygous clones labeled with GFP. (C) Repopulation is autonomously inhibited in Tr2. Small cells indicated by arrowheads are not included in a GFP-positive clone (arrow). (D) Ectopic repopulation is occasionally found in Tr3 (arrow). GFP, green; DAPI, magenta; DECad, white. Scale bar, 50 μm for (A, B), 17.5 μm for (C) and 35 μm for (D). (E) A schematic drawing illustrating possible roles of Hox/Hth/Exd complexes during repopulation. Prior to repopulation, Ubx/Hth/Exd and unknown factor X may act together to activate CycA and repress *fzr* expression to provide Tr2 larval cells with proliferative activity. Antp/Hth/Exd and Ubx/Hth/Exd may activate *fzr* and repress proliferative activity in Tr1 and Tr3, respectively.

but form the adult specific structures such as the head, thorax, wings and legs. An example of the imaginal anlagen that also participates in the larval life is the abdominal histoblasts that secrete both larval and adult cuticle (Fuse et al., 1994; Madhavan and Schneiderman, 1977; Ninov et al., 2007).

The results of our study revealed that small imaginal cells that go on to form the adult tracheal system are produced by rapid cell division of large larval cells in tracheal metamere Tr2, a process called "repopulation" (Guha and Kornberg, 2005). Although cells in Tr2 are large and morphologically very similar to larval cells in other metameres prior to repopulation, they are suggested to be proliferative diploid cells throughout larval development as visualized by marker expression (Figs. 4A and 7A, B). In contrast, Tr1/3 cells (and probably cells in more posterior metameres) are most probably in endocycles during larval life. Quantification of relative DNA amount also suggested Tr1/3 cells start endoreplication at first instar, while Tr2 cells remain diploid (Figs. 4C–E). We directly visualized sequential division of large cells in Tr2 during third instar (Figs. 5A, B). Results of a series of clonal analyses strongly support the idea that Tr2 cells stop proliferation after embryogenesis but re-proliferate in the course of repopulation during third larval instar (Figs. 5C–E). Since our findings clearly showed larval tracheal cells are not replaced by imaginal cells but re-proliferate to produce imaginal tracheal cells, the phenomenon should be called "reproliferation" instead of "repopulation".

It would be feasible to speculate cells in Tr2 branches secrete cuticle to form the tracheal luminal structures for both larva and adult, since at least parts of Tr2 branches (e.g. DTs) are preserved in the adult thorax (Manning and Krasnow, 1993). In this respect, the strategy of tracheal metamorphosis may be similar to that of abdominal histoblasts. However, the imaginal tracheal cells do not merely contribute to the adult DTs, but also respond to Bnl-FGF by migrating out of the larval system to form completely novel structures in the adult, the air sacs (Sato and Kornberg, 2002). Thus, the tracheal system may have characteristics of both imaginal discs and abdominal histoblasts as to the strategy of metamorphosis.

During metamorphosis of holometabolous insects, cells in larval structures contribute to adult structures in more ancestral species, while adult structures are formed via specialized primordia distinct from larval cells in more derived species (Svacha, 1992). For example, during metamorphosis of the legs in the beetle *Tenebrio molitor*, the entire larval leg epidermis contributes to the adult leg (Huet and Lenoir-Rousseaux, 1976). In the tobacco hornworm *Manduca sexta*, the adult primordia constitute specific parts of epidermal cells in the larval leg (Tanaka and Truman, 2005). The most derived mode of leg development is observed in *D. melanogaster*, in which the adult leg primordia are set-aside as an imaginal leg disc during larval development. Thus, production of imaginal cells from larval cells described in the present study may not be common in the most derived species such as *D. melanogaster*. However, similar strategies may be used to build adult structures of more ancestral holometabolous insects. Thus, the mechanisms of production of imaginal tracheal cells from larval cells and of subsequent formation of the air sacs in *Drosophila* may model formation of the adult structures in wide variety of holometabolous insects that utilize ancestral mode of metamorphosis. It will be interesting to see if similar strategies are used during metamorphosis of other holometabolous insects.

Acknowledgments

We thank Yumiko Kobayashi and Yuko Maeyama for technical assistance. We thank Kuniaki Takahashi, Kaoru Saigo and Ryu Ueda for UAS-IR library, Ken-ichi Takeyama and Shigeaki Kato for the use of confocal microscope, Shigeo Hayashi, Tetsuya Kojima, Ryo Matsuda and Chie Hosono for critical comments on the manuscript, Arjun Guha and Tom Kornberg for sharing results prior to publication. We are grateful to Barry Dickson, Tetsuya Kojima, Erina Kuranaga, Christian Lehner, Richard Mann, Masayuki Miura, Pat O'Farrell, Kaoru Saigo, Adi Salzberg, Yuki Takei-Yamaguchi, Rob White, NIG-FLY, the Vienna *Drosophila* RNAi Center, the Bloomington Stock Center, the *Drosophila* Genetic Resource Center, Kyoto and the Developmental Studies Hybridoma Bank for antibodies, fly strains and plasmids. This work was supported by Grants-in-Aid from the Ministry of Education, Science, and Culture of Japan (to M.S. and T.T.) and Kato Memorial Bioscience Foundation (to M.S.).

References

Cabernard, C., Affolter, M., 2005. Distinct roles for two receptor tyrosine kinases in epithelial branching morphogenesis in Drosophila. Dev. Cell 9, 831–842.
de Nooij, J.C., et al., 1996. A cyclin-dependent kinase inhibitor, Dacapo, is necessary for timely exit from the cell cycle during Drosophila embryogenesis. Cell 87, 1237–1247.
Fuse, N., et al., 1994. Diploidy of Drosophila imaginal cells is maintained by a transcriptional repressor encoded by escargot. Genes Dev. 8, 2270–2281.
Guha, A., Kornberg, T.B., 2005. Tracheal branch repopulation precedes induction of the Drosophila dorsal air sac primordium. Dev. Biol. 287, 192–200.
Huet, C., Lenoir-Rousseaux, J.J., 1976. Etude de la mise en place de la patte imaginable de *Tenebrio molitor*. 1. Analyse expérimentale des processus de restauration au cours de la morphogenése. J. Embryol. Exp. Morphol. 35, 303–321.
Igaki, T., et al., 2002. Eiger, a TNF superfamily ligand that triggers the Drosophila JNK pathway. EMBO J. 21, 3009–3018.
Ito, K., et al., 1997. The Drosophila mushroom body is a quadruple structure of clonal units each of which contains a virtually identical set of neurones and glial cells. Development 124, 761–771.
Kondo, S., et al., 2006. DRONC coordinates cell death and compensatory proliferation. Mol. Cell. Biol. 26, 7258–7268.
Kurant, E., et al., 1998. Dorsotonals/homothorax, the Drosophila homologue of meis1, interacts with extradenticle in patterning of the embryonic PNS. Development 125, 1037–1048.
Lane, M.E., et al., 1996. Dacapo, a cyclin-dependent kinase inhibitor, stops cell proliferation during Drosophila development. Cell 87, 1225–1235.
Lee, T., Luo, L., 1999. Mosaic analysis with a repressible cell marker for studies of gene function in neuronal morphogenesis. Neuron 22, 451–461.
Lee, T., et al., 1999. Development of the Drosophila mushroom bodies: sequential generation of three distinct types of neurons from a neuroblast. Development 126, 4065–4076.
Lehner, C.F., O'Farrell, P.H., 1990. The roles of Drosophila cyclins A and B in mitotic control. Cell 61, 535–547.
Lewis, E.B., 1978. A gene complex controlling segmentation in Drosophila. Nature 276, 565–570.
Madhavan, M.M., Schneiderman, H.A., 1977. Histological analysis of the dynamics of growth of imaginal discs and histoblast nests during the larval development of *Drosophila melanogaster*. Roux's Arch. Dev. Biol. 183, 269–305.
Manning, G., Krasnow, M.A., 1993. Development of the *Drosophila* tracheal system. In: Martinez-Arias, A., Bate, M. (Eds.), The Development of *Drosophila*, vol. 1. Cold Spring Harbor Laboratory Press, Cold Spring Harbor, New York, pp. 609–685.
Martinez-Arias, A., et al., 1993. Development and patterning of the larval epidermis of *Drosophila*. In: Martinez-Arias, A., Bate, M. (Eds.), The Development of Drosophila, vol. 1. Cold Spring Harbor Laboratory Press, Cold Spring Harbor, New York, pp. 517–608.
Matsuno, T., 1990. Metamorphosis of tracheae in the pupal abdomen of a fruit fly, *Drosophila melanogaster*. Meigen. Appl. Entomol. Zool. (Jpn.) 34, 167–169.
Metzger, R.J., Krasnow, M.A., 1999. Genetic control of branching morphogenesis. Science 284, 1635–1639.
Nakato, H., et al., 2002. dally, a Drosophila member of the glypican family of integral membrane proteoglycans, affects cell cycle progression and morphogenesis via a Cyclin A-mediated process. J. Cell Sci. 115, 123–130.
Ninov, N., et al., 2007. Extrinsic and intrinsic mechanisms directing epithelial cell sheet replacement during Drosophila metamorphosis. Development 134, 367–379.
Ohshiro, T., Saigo, K., 1997. Transcriptional regulation of breathless FGF receptor gene by binding of TRACHEALESS/dARNT heterodimers to three central midline elements in Drosophila developing trachea. Development 124, 3975–3986.
Pai, C.Y., et al., 1998. The Homothorax homeoprotein activates the nuclear localization of another homeoprotein, extradenticle, and suppresses eye development in Drosophila. Genes Dev. 12, 435–446.
Rieckhof, G.E., et al., 1997. Nuclear translocation of extradenticle requires homothorax, which encodes an extradenticle-related homeodomain protein. Cell 91, 171–183.
Ryoo, H.D., et al., 1999. Regulation of Hox target genes by a DNA bound Homothorax/Hox/Extradenticle complex. Development 126, 5137–5148.
Samakovlis, C., et al., 1996. Development of the Drosophila tracheal system occurs by a series of morphologically distinct but genetically coupled branching events. Development 122, 1395–1407.
Sato, M., Kornberg, T.B., 2002. FGF is an essential mitogen and chemoattractant for the air sacs of the Drosophila tracheal system. Dev. Cell 3, 195–207.
Schaeffer, V., et al., 2004. Notch-dependent Fizzy-related/Hec1/Cdh1 expression is required for the mitotic-to-endocycle transition in Drosophila follicle cells. Curr. Biol. 14, 630–636.

Shiga, Y., et al., 1996. A nuclear GFP beta-galactosidase fusion protein as a marker for morphogenesis in living Drosophila. Dev. Growth Differ. 38, 99–106.
Sigrist, S.J., Lehner, C.F., 1997. Drosophila fizzy-related down-regulates mitotic cyclins and is required for cell proliferation arrest and entry into endocycles. Cell 90, 671–681.
Svacha, P., 1992. What are and what are not imaginal discs: reevaluation of some basic concepts (Insecta, Holometabola). Dev. Biol. 154, 101–117.
Tanaka, K., Truman, J.W., 2005. Development of the adult leg epidermis in *Manduca sexta*: contribution of different larval cell populations. Dev. Genes Evol. 215, 78–89.
White, R.A., Wilcox, M., 1984. Protein products of the bithorax complex in Drosophila. Cell 39, 163–171.
Zhou, L., et al., 1997. Cooperative functions of the reaper and head involution defective genes in the programmed cell death of Drosophila central nervous system midline cells. Proc. Natl. Acad. Sci. U. S. A. 94, 5131–5136.